Evidence for cosmic evolution in the spin of the most massive black holes

Alejo Martínez-Sansigre[1,2,3*], Steve Rawlings[2]

[1] *Institute of Cosmology and Gravitation, University of Portsmouth, Dennis Sciama Building, Burnaby Road, Portsmouth, PO1 3FX, United Kingdom*
[2] *Astrophysics, Department of Physics, University of Oxford, Keble Road, Oxford OX1 3RH, United Kingdom*
[3] *SEPnet, South-East Physics network*

ABSTRACT

We use results from simulations of the production of magnetohydrodynamic jets around black holes to derive the cosmic spin history of the most massive black holes. We assume that the efficiency of jet production is a monotonic function of spin $\hat{a}$, as given by the simulations, and that the accretion flow geometry is similarly thick for quasars accreting close to the Eddington ratio and for low-excitation radio galaxies accreting at very small Eddington rates. We use the ratio of the comoving densities of the jet power and the radiated accretion power associated with supermassive black holes with $m_\bullet \gtrsim 10^8$ M$_\odot$ to estimate the cosmic history of the characteristic spin $\hat{a}$. The evolution of this ratio, which increases with decreasing z, is consistent with a picture where the $z \sim 0$ active galactic nuclei have typically higher spins than those at $z \sim 2$ (with typical values $\hat{a} \sim 0.35$-0.95 and $\hat{a} \sim 0.0$-0.25 respectively). We discuss the implications in terms of the relative importance of accretion and mergers in the growth of supermassive black holes with $m_\bullet \gtrsim 10^8$ M$_\odot$.

Key words: galaxies : active galaxies : jets–galaxies: nuclei – quasars: general –black hole physics – cosmology: miscellaneous

1 INTRODUCTION

Astrophysical black holes are described by two parameters, mass $m_\bullet$ and spin $\hat{a}$, defining the structure of space-time within regions close to the event horizon. Every massive galaxy has a supermassive black hole (SMBH) at its centre, and the combination of accretion and coalescence of SMBHs of similar mass, major merging, can lead to a wide spread in spins (e.g. Berti & Volonteri 2008). A possible constraint on the cosmic spin history is the ratio of kinetic to radiated outputs in active galactic nuclei (AGNs), since these are powered by SMBHs.

During accretion onto black holes, the amount of energy available for radiation and for the production of jets is determined by the mass and spin of the black hole, as well as the rate of accretion of matter and the geometry of the accretion flow. More massive black holes can accrete more matter, but those that are spinning rapidly can extract energy more efficiently from the infalling material (e.g. Novikov & Thorne 1973; Blandford & Znajek 1977). In addition, geometrically-thick accretion flows can power jets more effectively than thin ones because they are able to sustain more powerful poloidal magnetic fields (e.g. Meier 2001).

In galactic black holes (GBHs), the presence of steady jets occurs typically during low accretion rates (where by low we mean an Eddington ratio $\lambda \equiv \dot{m}/\dot{m}_{\rm Edd} \lesssim 10^{-2}$). During transitions to moderate accretion rates, $\lambda \gtrsim 10^{-2}$ the jet

is temporarily enhanced in power, and can then become steady, transient or totally absent (Fender et al. 2004). This is interpreted as a transition from advection-dominated accretion flows (ADAFs Narayan & Yi 1995) that are geometrically thick and can sustain significant jets, to gas-pressure-dominated accretion flows which are thin, with aspect ratios (the ratio of height to radius) ~ 0.01 (Novikov & Thorne 1973).

Quasars and high-excitation radio galaxies are SMBHs accreting at a high fraction of their Eddington limiting luminosity, so that the accretion flow is geometrically thick (Novikov & Thorne 1973, note GBHs with $\lambda \sim 1$ also produce continous jets, e.g. GRS 1915+105, Fender et al. 2004). Low-excitation radio galaxies are SMBHs with very low accretion rates, ADAFs, that have similarly thick accretion flows. The geometry is thus similar at both high and low accretion rates.

SMBHs are known to display a wide range of jet powers with no observable differences in the accretion flow, suggesting that a hidden variable must be controlling the jet power. The 'spin paradigm' assumes the black hole spin to be the physical parameter controlling the kinetic output in the form of jets (e.g. Blandford & Znajek 1977; Sikora et al. 2007).

GBHs show a similar wide spread in jet powers, but these are not found to correlate with the published estimates of the spins (Fender et al. 2010). If the spin estimates are correct, this provides very stringent evidence against the spin paradigm for GBHs. However, due to the uncertainties in the measurements of both the black

* alejo.martinez-sansigre@port.ac.uk

hole spin and the total jet power, the results found by Fender et al. (2010) do not provide robust evidence against the spin paradigm. The reader is referred to Section 7.2 of Martínez-Sansigre & Rawlings (2011, hereafter MSR11) for a detailed discussion.

In this letter we make the assumption that spin is indeed an important factor in powering jets, following the results of general-relativistic magnetohydrodynamic simulations (e.g. Hawley & Krolik 2006). Hence, assuming the spin paradigm to be correct, we present an observational constraint on the evolution of the mean spin of the most massive SMBHs as inferred from a measured cosmic change in the ratio of the power output in jets to the power radiated by active galactic nuclei (AGNs). We adopt a ΛCDM cosmology with the following parameters: $h = H_0/(100 \text{ km s}^{-1} \text{ Mpc}^{-1}) = 0.7$; $\Omega_m = 0.3$; $\Omega_\Lambda = 0.7$.

2   ASSUMPTIONS

High accretion rates will lead to efficient radiation of the thermal energy originating from viscous forces caused by magnetohydrodynamic turbulence. A fraction ϵ of the accreted energy will be radiated away, and the remaining energy will be advected into the black hole. The bolometric power available for radiation can therefore be described by:

$$L_{bol} = \epsilon \dot{m}_\bullet c^2 \qquad (1)$$

where L_{bol} is the bolometric luminosity due to radiation, $\dot{m}_\bullet$ is the rate of accretion of mass onto the SMBH, and the term ϵ is the radiative efficiency.

The shearing of magnetic fields frozen into the accreting plasma will allow the extraction of electromagnetic energy to power jets. Close to a rotating black hole, the dragging of inertial frames will lead to a higher angular velocity (and hence larger shear) and additional amplification of the magnetic fields occurs by extraction of energy from the rotating black hole. The power available for the production of jets can be described as:

$$Q_{jet} = \eta \dot{m}_\bullet c^2 \qquad (2)$$

where Q_{jet} is the jet power and η is the jet efficiency (e.g. Hawley & Krolik 2006, this is also the same as ϵ_{kin} in Merloni & Heinz 2008). Here it is assumed that η is a function of spin so that rapidly spinning black holes will have a higher jet efficiency.

The AGNs concerned in this letter are powered by SMBHs accreting either at very low or at very high fractions of their Eddington limiting luminosity (so either $\lambda \lesssim 10^{-2}$ or $\lambda \sim 1$ Willott et al. 2001; McLure et al. 2004; Smolčić et al. 2009). In these two limits of low- and high-accretion rates the geometry of the accretion flows will be similar, with aspect ratios $\gtrsim 0.1$. Hence, we assume that η is a monotonic function of $\hat{a}$ and that variations due to the accretion flow thickness are a secondary effect (see also Section 2.2 of MSR11 for more details).

3   THE COMOVING JET POWER AND RADIATED ENERGY

To infer the cosmic spin history of SMBHs, we will use the mean comoving kinetic jet power density from AGNs pro-

ducing jets, $\rho_{Q_{jet}}$, and the mean comoving jet power from radiating AGNs, $\rho_{L_{bol}}$. These quantities can both be measured using:

$$\rho_{Q_{jet}} = \int Q_{jet} \phi_{Q_{jet}}(Q_{jet}, z) \mathrm{d}Q_{jet} \qquad (3)$$

$$\rho_{L_{bol}} = \int L_{bol} \phi_{L_{bol}}(L_{bol}, z) \mathrm{d}L_{bol}, \qquad (4)$$

where $\phi_{Q_{jet}}(Q_{jet}, z) = \mathrm{d}^2 N/\mathrm{d}Q_{jet}\mathrm{d}z$ and $\phi_{L_{bol}}(L_{bol}, z) = \mathrm{d}^2 N/\mathrm{d}L_{bol}\mathrm{d}z$ are the luminosity functions for Q_{jet} and L_{bol} respectively, representing the comoving number density of AGNs with a given kinetic jet power or bolometric luminosity, and their evolution with cosmological redshift z

The jet power can be estimated from the low-frequency radio luminosity density due to synchrotron radiation (e.g. Willott et al. 1999), assuming that the jet output results in energy stored in radio source lobes together with associated and ineluctable work done on the source environment. Adopting standard assumptions for the way this energy is shared between magnetic fields and particles, the work done inflating these lobes as well as typical jet advance speeds and a typical density profile for the intergalactic medium, $\rho_{Q_{jet}}$ can be estimated from the radio luminosity function $\phi_{L_\nu}(L_\nu, z)$:

$$\left(\frac{\rho_{Q_{jet}}}{\text{W Mpc}^{-3}}\right) = 3 \times 10^{38} f^{\frac{3}{2}} \int \left(\frac{L_\nu}{10^{28}}\right)^{\frac{6}{7}} \phi_{L_\nu}(L_\nu, z) \mathrm{d}L_\nu, \quad (5)$$

where L_ν is the luminosity density at 151 MHz in W Hz^{-1} sr^{-1}. The term f represents the combination of several uncertainty terms when estimating Q_{jet} from L_ν (for example plasma volume filling factor or the fraction of energy in non-radiating particles). An alternative method to estimating jet powers is to estimate the energy stored in cavities in the X-ray emitting intra-cluster gas, and both methods agree best for $f \sim 20$ (Cavagnolo et al. 2010). We therefore initially take $f=20$ but in Section 4 consider deviations from this assumption.

The radio luminosity function includes two components: the luminosity function for the high radio luminosity classical double sources (Willott et al. 2001) and the luminosity function for the lower radio luminosity AGNs (Smolčić et al. 2009)[1]. For the lower radio luminosity AGNs, the luminosity function extends to $z=1.4$ only, and we have extrapolated it to $z=2.0$ using the same functional form for the evolution. The luminosity functions of other AGNs suggest a turnover around $z=2$, so no further extrapolation is attempted. We neglect any errors in the quantity inside the integral in Equation 5 which is reasonable because it is essentially the luminosity density, a quantity dominated by objects near the break in the radio luminosity function: the normalization at this break is directly measured to $z \sim 2$ (Willott et al. 2001; Vardoulaki et al. 2010).

In AGNs the hard (high-energy) X-ray luminosity originates from inverse-Compton scattering of photons from the accretion flow by a corona of hot electrons and it is a good tracer of the bolometric luminosity. The X-ray luminosity

---

[1] The latter has been converted from 1.4 GHz to 151 MHz assuming $L_\nu \propto \nu^{-\alpha}$ with a radio spectral index of $\alpha=0.75$

function $\phi_{L_\mathrm{X}}(L_\mathrm{X}, z)$ (Silverman et al. 2008) can be used to estimate ρ_{L_bol}:

$$\left(\frac{\rho_{L_\mathrm{bol}}}{\mathrm{W~Mpc^{-3}}}\right) = \int (1 + F_\mathrm{CT})\, C_\mathrm{X} L_\mathrm{X}\ \phi_{L_\mathrm{X}}(L_\mathrm{X}, z) \mathrm{d}L_\mathrm{X}. \quad (6)$$

The factor F_CT accounts for the fraction of luminous Compton-thick AGNs missed by the hard X-ray surveys: ($F_\mathrm{CT}\approx0.5$, e.g. Martínez-Sansigre et al. 2007; Gilli et al. 2007), and we adopt an uncertainty (from Table 8 of Fiore et al. 2009). so that $F_\mathrm{CT} = 0.5 \pm 0.1$. The bolometric correction C_X converts from a monochromatic luminosity to a bolometric luminosity, $L_\mathrm{bol} = C_\mathrm{X} L_\mathrm{X}$: we use the values given by (Hopkins et al. 2007) with, following Martínez-Sansigre & Taylor (2009), an assumed 8 per cent uncertainty.

The value of ρ_{Q_jet} is always dominated by the output from the most massive SMBHs, with $m_\bullet \gtrsim 10^8$ M$_\odot$ at all redshifts (McLure et al. 2004; Smolčić et al. 2009). To ensure that ρ_{L_bol} is also dominated by the most massive black holes, we only integrate above X-ray luminosities that can be achieved by SMBHs with $m_\bullet \geqslant 10^8$ M$_\odot$ accreting at $\geqslant 25\%$ of the Eddington accretion rate. This is a compromise between completeness to SMBHs with $m_\bullet \geqslant 10^8$ M$_\odot$ and contamination from lower-mass SMBHs. This value securely avoids serious contamination from SMBHs with masses $<10^8$ M$_\odot$. From the distribution in λ found by Heckman et al. (2004, their Figure 3) we estimate that it leads to ρ_{L_bol} at low-z being underestimated by a factor ~3. At high redshift we expect it to underestimate ρ_{L_bol} by a negligible amount.

This evolution of the ratio $\rho_{Q_\mathrm{jet}}/\rho_{L_\mathrm{bol}}$ with redshift z for the most massive SMBHs (with $m_\bullet \gtrsim 10^8$ M$_\odot$) is shown in Figure 1. There is likely some exaggeration of the rise in $\rho_{Q_\mathrm{jet}}/\rho_{L_\mathrm{bol}}$ towards low z, because of the cut-off assumed in X-ray luminosity, but only by a factor ~0.5 (base-10 logarithm), smaller than the inferred cosmic rise towards low z. Note also that the absolute value of the height of the curve will scale with f as $f^{3/2}$.

4 THE COSMIC SPIN HISTORY

The ratio of ρ_{Q_jet} and ρ_{L_bol}, for the most massive black holes ($\gtrsim 10^8$ M$_\odot$) is then given by

$$\frac{\rho_{Q_\mathrm{jet}}}{\rho_{L_\mathrm{bol}}} = \frac{\eta \rho_{\dot{m}_\bullet Q_\mathrm{jet}}}{\epsilon \rho_{\dot{m}_\bullet L_\mathrm{bol}}}, \quad (7)$$

that includes the comoving density of accretion of the AGNs contributing to ρ_{Q_jet}, namely $\rho_{\dot{m}_\bullet Q_\mathrm{jet}}$ and of AGNs contributing to ρ_{L_bol}, namely $\rho_{\dot{m}_\bullet L_\mathrm{bol}}$.

Separating the contribution to ρ_{Q_jet} from ADAFs and quasars, $\rho_{Q_\mathrm{jet}} = \eta_\mathrm{ADAF} \rho_{\dot{m}_\mathrm{ADAF}} + \eta_\mathrm{QSO} \rho_{\dot{m}_\mathrm{QSO}}$. In the case of ρ_{L_bol}, although $\rho_{\dot{m}_\mathrm{ADAF}} \ll \rho_{\dot{m}_\mathrm{QSO}}$, $\epsilon_\mathrm{ADAF} \ll \epsilon_\mathrm{QSO}$, so that ρ_{L_bol} is totally dominated by quasars and $\rho_{L_\mathrm{bol}} = \epsilon_\mathrm{QSO} \rho_{\dot{m}_\mathrm{QSO}}$.

Hence,

$$\frac{\rho_{Q_\mathrm{jet}}}{\rho_{L_\mathrm{bol}}} = \left(\frac{\eta_\mathrm{ADAF}}{\epsilon_\mathrm{QSO}}\right)\left(\frac{\rho_{\dot{m}_\mathrm{ADAF}}}{\rho_{\dot{m}_\mathrm{QSO}}}\right) + \left(\frac{\eta_\mathrm{QSO}}{\epsilon_\mathrm{QSO}}\right). \quad (8)$$

We consider two approaches to using $\rho_{Q_\mathrm{jet}}/\rho_{L_\mathrm{bol}}$ to constrain the cosmic spin history. The first one is to attempt to use the ratio to find a fiducial spin, under some simplifying assumptions. The second is to compare a parametric model to the observations, to see how well it reproduces them.
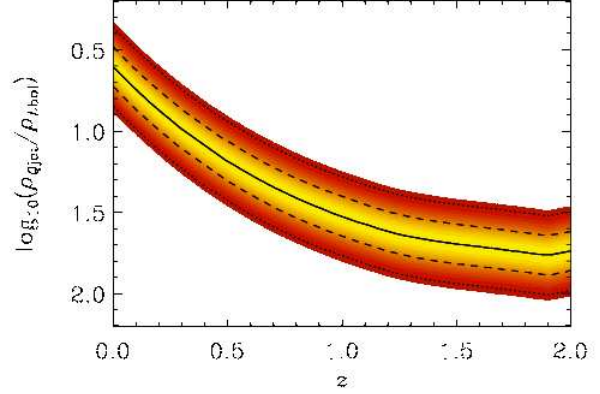
Figure 1. The posterior probability distribution function for the logarithm (base 10) of $\rho_{Q_\mathrm{jet}}/\rho_{L_\mathrm{bol}}$ as a function of redshift for the most massive black holes (with $m_\bullet \gtrsim 10^8$ M$_\odot$). The colours represent the normalised posterior probability of $\rho_{Q_\mathrm{jet}}/\rho_{L_\mathrm{bol}}$, given the data. Light yellow represents the highest probabilities, dark red the lowest. Contours are also marked as black lines, including the line of maximum posterior probability (solid), as well as the $\pm 1\sigma$ (dashed) and $\pm 2\sigma$ (dotted) lines. At all redshifts we only integrate above X-ray luminosities that can be achieved by SMBHs with $m_\bullet \geqslant 10^8$ M$_\odot$ accreting at $\geqslant 25\%$ of the Eddington accretion rate (the characteristic value found by McLure & Dunlop 2004).

In both approaches, the jet efficiency η is described using the results from a set of three-dimensional general-relativistic magnetohydrodynamic simulations, which can be approximated as (Hawley & Krolik 2006):

$$\eta(|\hat{a}|) \approx 0.002\,(1 - |\hat{a}|)^{-1}. \quad (9)$$

For spin values $\hat{a} = [0.0, 0.5, 0.998]$ the corresponding jet efficiencies are $\eta = [0.002, 0.004, 1.00]$. However, our results are very similar if we use other efficiencies from the literature (see supplementary figures and MSR11).

For the radiative efficiency, we assume the Novikov & Thorne (1973) model, which for spins $\hat{a} = [0.0, 0.5, 0.998]$ has values $\epsilon = [0.057, 0.082, 0.321]$ for co-rotating accretion[2].

4.1 The fiducial cosmic spin

At $z \gtrsim 1$, the density of accretion onto ADAFs is insignificant compared to the density of accretion onto quasars (e.g. see Figure 9 of MSR11 and Figure 4 of Merloni & Heinz 2008), $\rho_{\dot{m}_\mathrm{ADAF}} \ll \rho_{\dot{m}_\mathrm{QSO}}$ so that $\rho_{Q_\mathrm{jet}}/\rho_{L_\mathrm{bol}} = \eta_\mathrm{QSO}/\epsilon_\mathrm{QSO}$. Therefore, at high redshift $\rho_{Q_\mathrm{jet}}/\rho_{L_\mathrm{bol}}$ gives a good estimate of the

---

[2] In Section 5, we will discuss the relevance of chaotic accretion. In this paradigm, an average efficiency of co- and counter-rotating accretion should be used (King et al. 2008). The results of MSR11 used jet efficiencies from the literature for co-rotating accretion, so for consistency we limit ourselves to these. The radiative efficiency is determined for quasars and their spins are close to $\hat{a}=0.0$ (MSR11) so the co- and counter-rotating radiative efficiencies are virtually identical. Therefore, although there is a slight conceptual inconsistency between our model radiative efficiency and our interpretation, in practice it makes no difference to the results.

ratio of efficiencies for quasars and, under the spin paradigm, of their typical spin.

At very low redshifts the comoving density of accretion onto ADAFs is comparable to that of quasars, so $\rho_{\dot{m}_{\rm ADAF}} \approx \rho_{\dot{m}_{\rm QSO}}$ (Merloni & Heinz 2008, MSR11), in which case $\rho_{Q_{\rm jet}}/\rho_{L_{\rm bol}} \approx (\eta_{\rm ADAF}/\eta_{\rm QSO} + 1)\eta_{\rm QSO}/\epsilon_{\rm QSO}$. It is therefore not straightforward to interpret $\rho_{Q_{\rm jet}}/\rho_{L_{\rm bol}}$ in terms of typical efficiencies, but some progress can be made under the assumption that $\eta_{\rm ADAF} \gtrsim \eta_{\rm QSO}$, so that $\rho_{Q_{\rm jet}}/\rho_{L_{\rm bol}} \gtrsim 2\eta_{\rm QSO}/\epsilon_{\rm QSO}$. This shows that at $z \sim 0$ the ratio $\rho_{Q_{\rm jet}}/\rho_{L_{\rm bol}}$ will overestimate the typical efficiencies of quasars and ADAFs.

Figure 2 represents a fiducial cosmic spin history of the most massive black holes inferred from $\rho_{Q_{\rm jet}}/\rho_{L_{\rm bol}}$. It represents the characteristic spin if at a given redshift all SMBHs have the same spin. It is derived by assuming the first term in Equation 8 is negligible, so we expect this figure to provide an accurate estimate at moderate and high redshifts, but to overpredict $\hat{a}_{\rm fid}(z)$ at the low redshifts, marked in gray. Overestimating η/ϵ by a factor of >2 at $z \sim 0$ suggests that the typical spin at $z \sim 0$ is <0.9 rather than ~ 0.95. Consideration of f suggests that lower values of f also lead to lower estimates of the typical low-z spin: re-running our analysis with $f = 10$ (rather than $f = 20$) leads to no changes at high z but a typical low-z spin of 0.8. We note that high values of f are supported by X-ray cavity observations undertaken at low radio powers and low redshift so lower values of f for the low-z population are hard to envisage. If we assume that different effects (e.g. f and underestimating $\rho_{L_{\rm bol}}$ at low-z) add to an overall overestimate of $\rho_{Q_{\rm jet}}/\rho_{L_{\rm bol}}$ by a factor of ~ 2 (4), this will result in a fiducial spin at $z \sim 0$ of $\hat{a}_{\rm fid} \sim 0.9$ (0.7). In these cases the inferred evolution would be less extreme, but still present.

To test wether this fiducial spin history is consistent with constraints from the radiative efficiency of quasars (the Sołtan 1982, argument), we compute the luminosity-weighted spin (see also MSR11): $\langle \hat{a} \rangle_{\rm L} \equiv \int \hat{a}_{\rm fid}(z)\rho_{L_{\rm bol}}dz / \int \rho_{L_{\rm bol}}dz$. The spin history of Fig. 2 yields a luminosity-weighted spin is $\langle \hat{a} \rangle_{\rm L} = 0.055$, which corresponds to a radiative efficiency of $\langle \epsilon \rangle_{\rm L} = 0.059$. This is in good agreement with observational constraints, which typically yield values $\langle \epsilon \rangle_{\rm L} \sim 0.05$-$0.10$ (see e.g. Martínez-Sansigre & Taylor 2009).

4.2 Can we explain $\rho_{Q_{\rm jet}}/\rho_{L_{\rm bol}}$?

In MSR11, we inferred a moderate evolution amongst the SMBHs with $m_{\bullet} \geqslant 10^8$ M$_{\odot}$. This evolution was really driven by the change in relative space densities of two populations: the high Eddington-rate SMBHs, or quasars, which dominate at high redshifts, were found to have spin distributions centred around low spin, $\hat{a} \sim 0$. The low Eddington-rate SMBHs, or ADAFs, become significant at low redshifts, and these were found to have a bimodal spin distribution, with a peak centred at $\hat{a} \sim 0$ and another at $\hat{a} \sim 1$. These spin distributions allowed us to explain the local radio luminosity function, as well as explaining its evolution up to $z \sim 1$.

The results of MSR11 suggest that the evolution of the mean spin of SMBHs is driven by a transition from a high-accretion rate, low spin population, to a low-accretion rate population showing a bimodality in spins (and hence a slightly higher mean spin). This evolution was qualita-
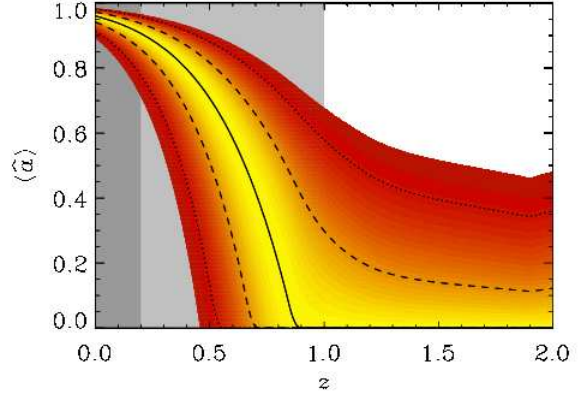

Figure 2. Fiducial spin of the most massive black holes as a function of redshift. It shows the posterior probability distribution for $\hat{a}_{\rm fid}(z)$ given the ratio $\rho_{Q_{\rm jet}}/\rho_{L_{\rm bol}}$ plotted in Figure 1, given $\eta(|\hat{a}|)$ and $\epsilon(|\hat{a}|)$. The posterior probability has been normalised at each redshift. The underlying assumption is that the aspect ratio of the accretion flow is similar for all the AGNs contributing to $\rho_{Q_{\rm jet}}/\rho_{L_{\rm bol}}$, so that geometry has a negligible effect in the evolution of $\rho_{Q_{\rm jet}}/\rho_{L_{\rm bol}}$, which is determined by the evolution in cosmic spin. The colours and contours are the same as those in Figure 1. At $z \gtrsim 0.9$, the maximum posterior probability line as well as the -1 and -2σ contours go along the $\hat{a}=0$ axis. The grey shades mark the regions where the assumption that $\rho_{\dot{m}_{\rm ADAF}} \ll \rho_{\dot{m}_{\rm QSO}}$ breaks down. In the light gray region, we estimate that $\rho_{\dot{m}_{\rm ADAF}} \approx 0.1\rho_{\dot{m}_{\rm QSO}}$ while in the dark gray region, $\rho_{\dot{m}_{\rm ADAF}} \approx 0.25\rho_{\dot{m}_{\rm QSO}}$ (MSR11). Hence in these regions we overestimate $\hat{a}_{\rm fid}(z)$.

tively similar to that seen in Fig. 2, but it was significantly weaker, changing from $\langle \hat{a} \rangle \sim 0.25$ at high redshift to ~ 0.35 at low redshift.

We can test whether the spin distributions we inferred in MSR11 can reproduce the observed evolution in $\rho_{Q_{\rm jet}}/\rho_{L_{\rm bol}}$. We use these spin distributions to predict how the ratio $\rho_{Q_{\rm jet}}/\rho_{L_{\rm bol}}$ evolves with redshift using

$$\left(\frac{\rho_{Q_{\rm jet}}}{\rho_{L_{\rm bol}}} \right)_{\rm pred} = \left(\frac{\langle \eta_{\rm ADAF} \rangle}{\langle \epsilon_{\rm QSO} \rangle} \right) \left(\frac{\rho_{\dot{m}_{\rm ADAF}}}{\rho_{\dot{m}_{\rm QSO}}} \right) + \left(\frac{\langle \eta_{\rm QSO} \rangle}{\langle \epsilon_{\rm QSO} \rangle} \right). (10)$$

Note that the angled brackets indicate expectation values: $\langle \eta_{\rm ADAF} \rangle = \int \eta(\hat{a})P_{\rm ADAF}(\hat{a})d\hat{a}$, $\langle \eta_{\rm QSO} \rangle = \int \eta(\hat{a})P_{\rm QSO}(\hat{a})d\hat{a}$ and $\langle \epsilon_{\rm QSO} \rangle = \int \epsilon(\hat{a})P_{\rm QSO}(\hat{a})d\hat{a}$. The variance of the ADAF term is large, due to the bimodal nature, while the variance of the QSO term is small. As mentioned earlier, at $z \gtrsim 1$ $\rho_{\dot{m}_{\rm QSO}} \gg \rho_{\dot{m}_{\rm ADAF}}$ so that the $\eta_{\rm QSO}$ term dominates, but at low redshift $\rho_{\dot{m}_{\rm QSO}} \sim \rho_{\dot{m}_{\rm ADAF}}$.

Fig. 3 shows the resulting evolution of $\rho_{Q_{\rm jet}}/\rho_{L_{\rm bol}}$, from Equation 10 and using the spin distributions from MSR11. At $z \sim 0$ the most likely predicted value of $\rho_{Q_{\rm jet}}/\rho_{L_{\rm bol}}$ is about 0.1 dex higher than the observed value, and at $z \gtrsim 1$ it is about 0.3 dex higher. This can be understood since in MSR11 (Figs. 4 and 7 of that work) we overpredicted the radio luminosity function of high-Eddington rate SMBHs, which dominate $\rho_{Q_{\rm jet}}$ at high redshifts.

The expectation value is systematically slightly higher than the most likely value of $\rho_{Q_{\rm jet}}/\rho_{L_{\rm bol}}$ shown in Fig. 1, but the curvature is similar and the two figures agree very well within their uncertainties. Similar results are found using
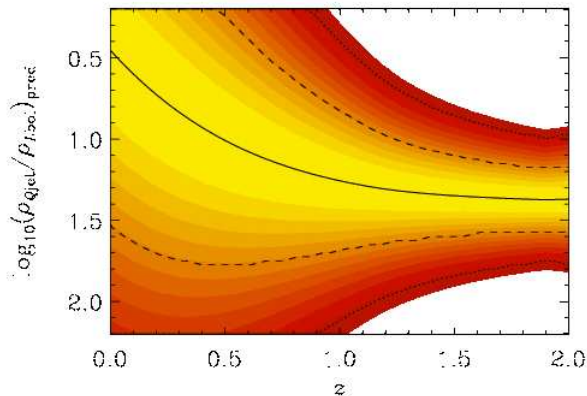
Figure 3. The evolution of $\rho_{Q_{jet}}/\rho_{L_{bol}}$ as predicted by the spin distributions from MSR11. In MSR11 we predicted spin distributions for high-Eddington rate objects (QSOs) and low-Eddington rate ones (ADAFs), as well as the accretion density onto these two sub-populations ($\rho_{\dot{m}_{QSO}}$ and $\rho_{\dot{m}_{ADAF}}$ respectively). Following Equations 8 and 10, and the spin distributions from MSR11, we predict an expectation value that behaves very similarly to that of Fig. 1. The contours are wide due to the variance of the spin probability distributions for high- and low-Eddington rate objects. At low redshifts the variance is larger due to the bimodality in the spin distribution of the low-Eddington rate objects.

other jet efficiencies from the literature (see supplementary figures).

Although the amount of evolution in the mean spin is different, Fig. 2 and the mean spin from MSR11, which can reproduce Fig. 1, agree qualitatively: the typical spin was very low at high redshifts, and has increased at low redshifts.

5 DISCUSSION

Using the observed ratio between the comoving densities of jet power and radiation from SMBHs, $\rho_{Q_{jet}}/\rho_{L_{bol}}$, we have inferred that the spin of the SMBHs must be evolving. We have done this in two ways. The first method included some simplifying assumptions to allow us to "invert" the problem. This allowed us to infer a fiducial spin for all SMBHs, and we find this fiducial spin evolves strongly. The second method consists of comparing some highly parametrised description of the spin distributions, inferred from fitting the local radio luminosity function in our previous work (MSR11). There are no simplifying assumptions, but rather than infer the evolution of a fiducial spin value, we simply test whether spin distributions previously inferred in MSR11 can explain the observed evolution of $\rho_{Q_{jet}}/\rho_{L_{bol}}$: we find that they can explain this evolution very well.

The results from both methods are quantitatively different, in that they differ in the spin values inferred at low redshift. However the two methods agree qualitatively: a low-spin epoch occurs at $z \gtrsim 1$ and coincides with the period during which the black holes with masses $m_\bullet \gtrsim 10^8$ M$_\odot$ accreted most of their mass (Yu & Tremaine 2002). This epoch is one characterised by high accretion rates onto low-spin objects, while the present-day epoch ($z \sim 0$) is characterised by

low accretion rates onto a population of SMBHs where a significant fraction have high spins.

Somewhat counter-intuitively, the epoch of lowest-spin corresponds to the epoch of highest accretion. This, however, is consistent instead with the paradigm of "chaotic accretion" (e.g. King et al. 2008): approximately half of the accretion occurs with the disc counter-rotating with respect to the SMBH, hence decreasing the spin of the hole as opposed to the increase brought by a co-rotating disc.

Chaotic accretion is expected to lead to SMBHs with low spins, $\hat{a} \sim 0.1$ (King et al. 2008), and our result is thus in agreement with black holes being "spun down" at high redshift, when the typical accretion rate was higher, due to the greater available supply of concentrated cold gas in the central regions of the host galaxy (e.g. Obreschkow & Rawlings 2009).

When two black holes of similar mass coalesce, the orbital angular momentum contributes significantly to the final angular momentum of the coalesced black hole, leading to high values of the final spin, typically $\hat{a} \sim 0.7$ (Rezzolla et al. 2008). Hence, mergers of SMBHs of similar mass (major mergers, with mass ratios $\lesssim 4:1$) are expected to provide the "spin-up" mechanism.

SMBHs of mass $\gtrsim 10^8$ M$_\odot$ are hosted by galaxies with bulge masses $\gtrsim 10^{11}$ M$_\odot$, typically elliptical galaxies. A significant fraction of these galaxies have undergone major mergers since $z \sim 1$ (Robaina et al. 2010), meaning their central SMBHs will have most likely undergone a major merger too.

Due to the steepness of the mass function above the break in the mass function, our result is most likely dominated by the behaviour of SMBHs hosted by galaxies with masses $\sim 1 \times 10^{11}$ M$_\odot$ and reflects their merger history, rather than reflecting that of the rarer, more massive galaxies with $> 3 \times 10^{11}$ M$_\odot$, which seem to have undergone an earlier evolution (Banerji et al. 2010).

The mechanism for spinning-up SMBHs, major merging, is present during the entire epoch of $0 \leqslant z \leqslant 2$ since the merging of galaxies with similar masses is also a common occurrence at redshifts $z \sim 2$. However, the centrally concentrated, typically molecular, cold gas content of the merging galaxies, the fuel for accretion, decreases significantly with cosmic time.

It is therefore the gradual disappearance of the "braking" mechanism, chaotic accretion, which determines the increase in the typical spin of the most massive black holes.

REFERENCES

Banerji M., Ferreras I., Abdalla F. B., Hewett P., Lahav O., 2010, MNRAS, 402, 2264
Berti E., Volonteri M., 2008, ApJ, 684, 822
Blandford R. D., Znajek R. L., 1977, MNRAS, 179, 433
Cavagnolo K. W., McNamara B. R., Nulsen P. E. J., Carilli C. L., Jones C., Bîrzan L., 2010, ApJ, 720, 1066

Croston J. H., Birkinshaw M., Hardcastle M. J., Worrall D. M., 2004, MNRAS, 353, 879

Fender R. P., Belloni T. M., Gallo E., 2004, MNRAS, 355, 1105

Fender R. P., Gallo E., Russell D., 2010, MNRAS, 406, 1425

Fiore F. et al. 2009, ApJ, 693, 447

Gilli R., Comastri A., Hasinger G., 2007, A&A, 463, 79

Hawley J. F., Krolik J. H., 2006, ApJ, 641, 103

Heckman T. M., Kauffmann G., Brinchmann J., Charlot S., Tremonti C., White S. D. M., 2004, ApJ, 613, 109

Hopkins P. F., Richards G. T., Hernquist L., 2007, ApJ, 654, 731

King A. R., Pringle J. E., Hofmann J. A., 2008, MNRAS, 385, 1621

Martínez-Sansigre A., Rawlings S., 2011, MNRAS, 414, 1937

Martínez-Sansigre A., et al., 2007, MNRAS, 379, L6

Martínez-Sansigre A., Taylor A. M., 2009, ApJ, 692, 964

McLure R. J., Dunlop J. S., 2004, MNRAS, 352, 1390

McLure R. J., Willott C. J., Jarvis M. J., Rawlings S., Hill G. J., Mitchell E., Dunlop J. S., Wold M., 2004, MNRAS, 351, 347

Meier D. L., 2001, ApJL, 548, L9

Merloni A., Heinz S., 2008, MNRAS, 388, 1011

Narayan R., Yi I., 1995, ApJ, 452, 710

Novikov I. D., Thorne K. S., 1973, in Black Holes, ed. C. Dewitt, & B. S. Dewitt (New York: Gordon and Breach), 343

Obreschkow D., Rawlings S., 2009, ApJL, 696, L129

Rezzolla L., Barausse E., Dorband E. N., Pollney D., Reisswig C., Seiler J., Husa S., 2008, Phys. Rev. D, 78, 044002

Robaina A. R., Bell E. F., van der Wel A., Somerville R. S., Skelton R. E., McIntosh D. H., Meisenheimer K., Wolf C., 2010, ApJ, 719, 844

Sikora M., Stawarz Ł., Lasota J.-P., 2007, ApJ, 658, 815

Silverman J. D., et al., 2008, ApJ, 679, 118

Smolčić V., et al., 2009, ApJ, 696, 24

Sołtan A., 1982, MNRAS, 200, 115

Vardoulaki E.., Rawlings S., Hill G. J., Mauch T., Inskip K. J, Riley J., Brand K., Croft S., Willott C. J. ., 2010, MNRAS, 401, 1709

Willott C. J., Rawlings S., Blundell K. M., Lacy M., 1999, MNRAS, 309, 1017

Willott C. J., Rawlings S., Blundell K. M., Lacy M., Eales S. A., 2001, MNRAS, 322, 536

Yu Q., Tremaine S., 2002, MNRAS, 335, 965